Supplementary Information

Microfluidic acoustic sawtooth metasurfaces for patterning and separation using traveling surface acoustic waves

Mingxin Xu, Peter VS Lee, David Collins*

Department of Biomedical Engineering, University of Melbourne, Melbourne, Victoria, Australia

* Corresponding author
E-mail: david.collins@unimelb.edu.au

Supplementary Note 1: Analytical formal and derivation for non-integer k values

As shown in Fig. S1(a), L_{div} is defined as the length of the fringe produced by a single sawtooth element (equals to the length of the hypotenuse of each triangle element), written as

$$L_{div} = \frac{h_{st}}{\sin \theta_{st}}, \qquad (S1)$$

Fig. S1(b) is the expanded view of Fig. S1(a). The distance between the two fringes is $k\lambda_\theta - h_\theta$, where the blue line represents the resulting divergent fringe. The angle at which the divergent fringe increases relative to θ_{st} is defined as θ_{inc}^{+}, which is calculated as:

$$\theta_{inc}^{+} = \tan^{-1}\left(\frac{k\lambda_\theta - h_\theta}{L_{div}}\right), \qquad (S2)$$

where $h_\theta = h_{st}\cos\theta_{st}$.

For $\theta_{div}^{+} = \theta_{st} + \theta_{inc}^{+}$ (superscript "+" denoting a θ_{div} is larger than θ_{st}), rewriting equations (S1) and (S2) with θ_{div}^{+}, this becomes

$$\theta_{div}^{+} = \theta_{st} + \theta_{inc}^{+} = \theta_{st} + \tan^{-1}\left(\frac{(k\lambda_\theta - h_\theta)\sin\theta_{st}}{h_{st}}\right) \qquad (S3)$$

Conversely, for θ_{div} slightly smaller than θ_{st}, this expression incorporating θ_{div}^{-} (superscript " − " for θ_{div} is slightly smaller than θ_{st}) is expressed as:

$$\theta_{div}^{-} = \theta_{st} - \theta_{inc}^{-} = \theta_{st} - \tan^{-1}\left(\frac{(h_\theta - k\lambda_\theta)\sin\theta_{st}}{h_{st}}\right). \qquad (S4)$$

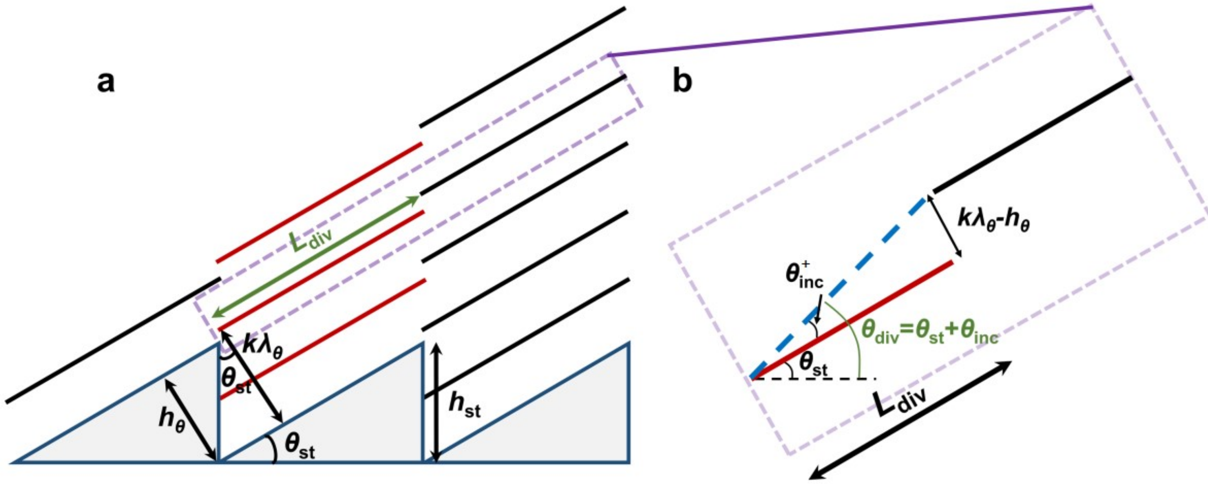

FIG. S1. Analytical approach for predicting the resulting θ_{div} where k is a non-integer value. (a) Here for $h_{\theta}^{-} \lesssim k\lambda_{\theta}$, with (b) showing an expanded analysis of these fringes.

The analytical results calculated based on equations (S3) and (S4) are shown in Fig. S2. Corresponding simulation results are shown in Fig. 2(b).

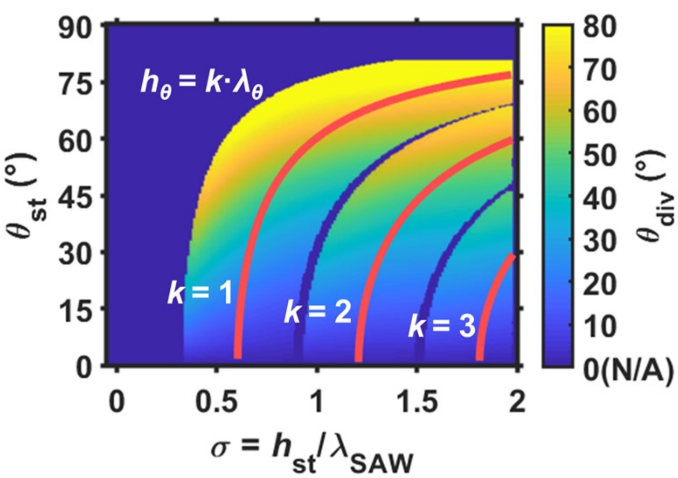

FIG. S2. Analytical modelling results, plotting θ_{div} as a function of θ_{st} and σ, overlaid with red lines corresponding to $k = 1$, $k = 2$ and $k = 3$.

Supplementary Note 2: Deriving generalized Snell's law for the proposed metasurfaces.

For acoustic waves that incident perpendicular to the metasurface (the incidence angle is 0), the generalized Snell's law of refraction is written as [1]:

$$\frac{1}{\lambda_\theta}\sin\left(\theta_t\right) = \frac{1}{2\pi}\frac{d\varphi(y)}{dy}, \tag{S5}$$

Where the fringe spacing λ_θ is described in equation (1), θ_t is the equivalent refraction angle (equal to θ_{div}) as shown in Fig. S3. dy is the length along the y axis for which the equivalent phase shift ($d\varphi(y)$) is equal to 2π.

As shown in Fig. S3, $dy = w_{st}/k$, where $w_{st} = \mathrm{h}_{st}/\tan\left(\theta_{st}\right)$. Therefore, dy is expressed as:

$$dy = \frac{h_{st}}{k\tan\left(\theta_{st}\right)}. \tag{S6}$$

Substituting equation (S6) into equation (S5) with $d\varphi(y) = 2\pi$, and rewriting equation (S5) yields the generalized Snell's law for our sawtooth metasurfaces:

$$\frac{1}{\lambda_\theta}\sin\left(\theta_{div}\right) = \frac{k\tan\left(\theta_{st}\right)}{h_{st}}, \tag{S7}$$

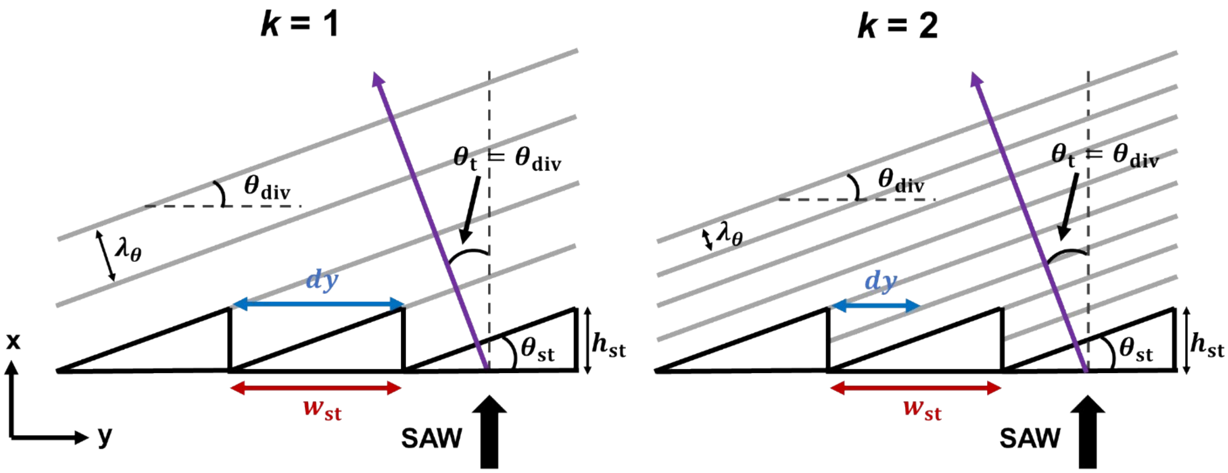

FIG. S3. Schematic diagram of deriving generalized Snell's law. For $k = 1$ and $k = 2$.

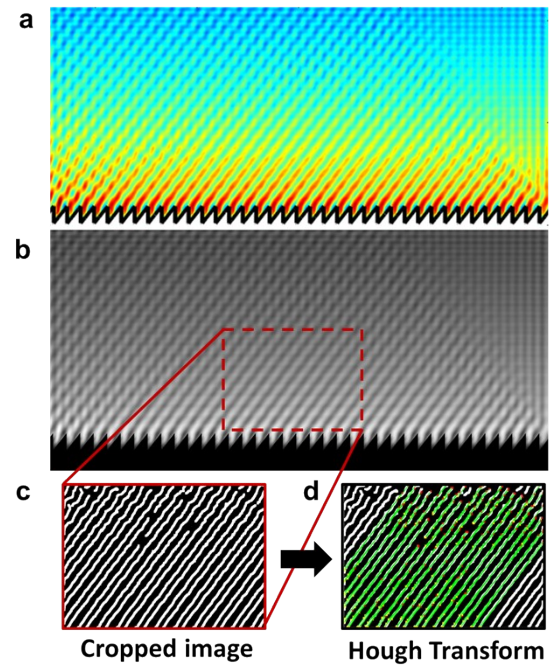

FIG. S4. Example of Hough transform with $\sigma = 0.84\ and\ \theta_{st} = 51.8$. (a) The simulated acoustic pressure field. (b) Grayscale remapping of acoustic pressure field. (c) A cropped image segment, where the edge features are detected by the edge function. (d) The lines are detected by the Hough transform, where the angle of each line can be extracted.

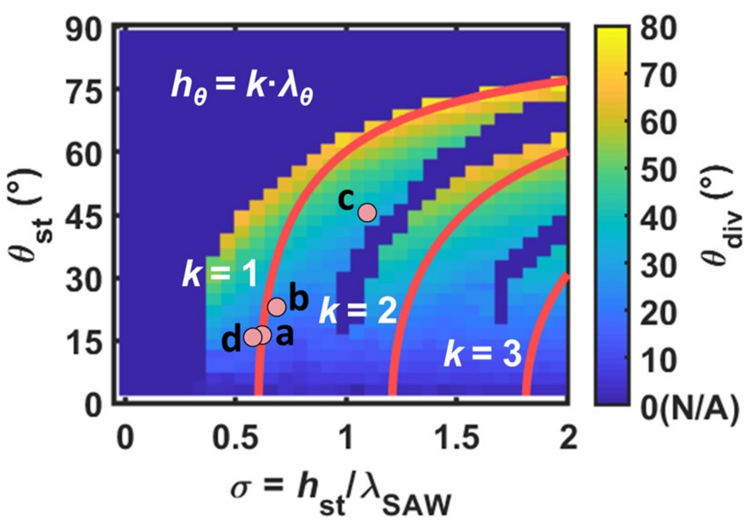

FIG. S5. Simulation results, where each marked point corresponds to the sub-figure number in Fig. 4.

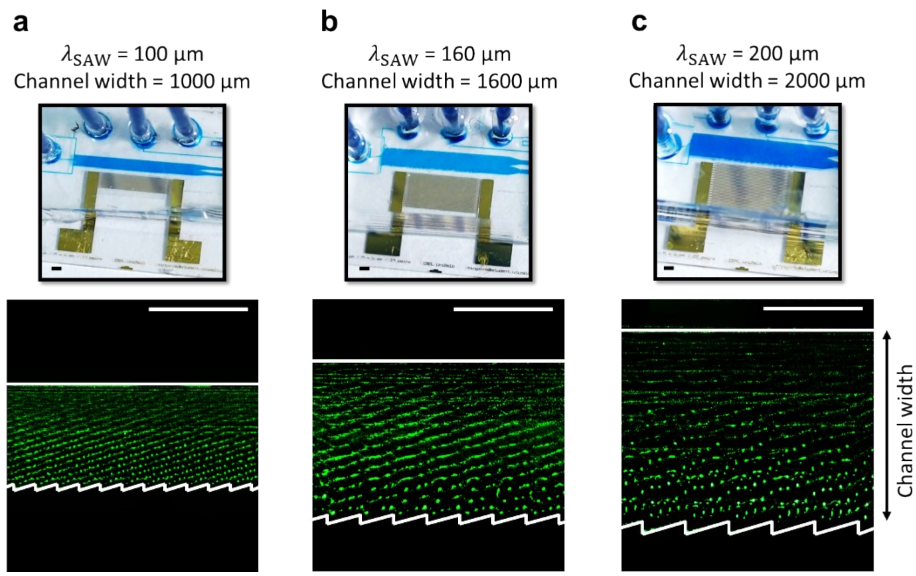

FIG. S6. Experimental results with various wavelengths and channel widths, where $h_{st} = 0.62\lambda_{SAW}, \theta_{st} = \theta_{div} = 16.2°,\ and\ k = 1$ for each design. (a) $\lambda_{SAW} = 100\ \mu m$ and $channel\ width = 1000\ \mu m$. (b) $\lambda_{SAW} = 160\ \mu m$ and $channel\ width = 1600\ \mu m$. (c) $\lambda_{SAW} = 200\ \mu m$ and $channel\ width = 2000\ \mu m$. Scale bars are 1000 µm.

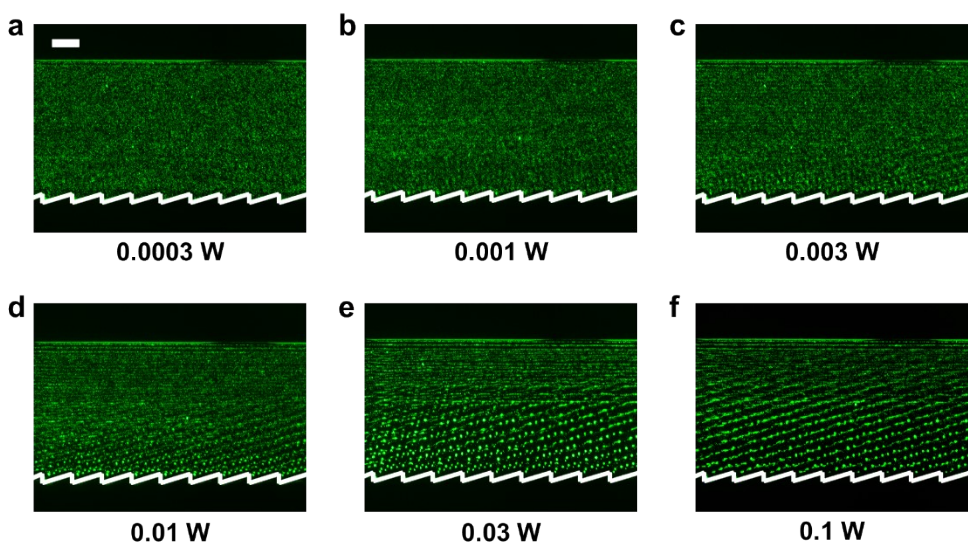

FIG. S7. Input power effects. Experimental results with $\lambda_{SAW} = 100\ \mu m$ $and\ k = 1$, for the input power of the transducer is (a) 0.0003 W, (b) 0.001 W, (c) 0.003 W, (d) 0.01 W, (e) 0.03 W, and (f) 0.1 W. Scale bars is 200 µm.

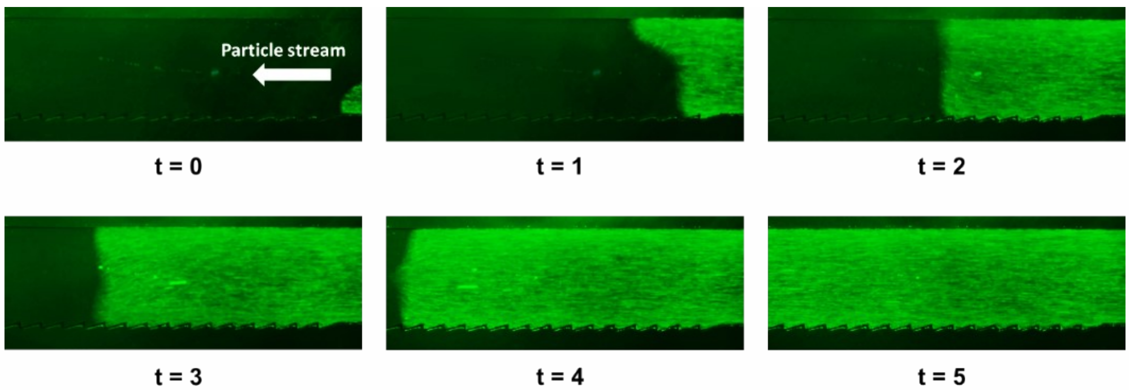

FIG. S8. Experimental results demonstrating filling without bubble formation at low perfusion flow rates (~ 7 µL/min).

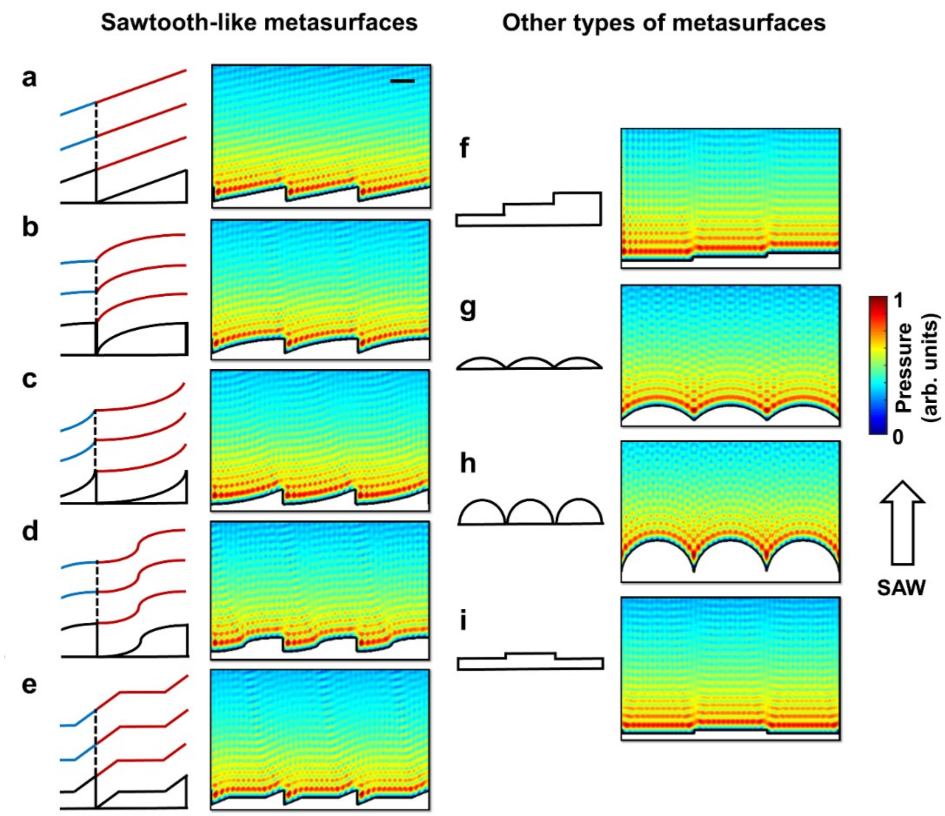

FIG. S9. Examples and acoustic pressure field simulations of sawtooth-like metasurfaces and other metasurfaces with $\lambda_{SAW} = 100\ \mu m$. (a)-(e) Sawtooth-like metasurfaces. The pattern generated by each sawtooth-like element has the same length at the dotted line to form spatially continuous patterns, where the spacing of the pattern at a given θ_{st} can be calculated by equation (1). (f)-(i) Other types of metasurfaces. Scale bar is $100\ \mu m$.

Reference

1. Tian Z, Shen C, Li J, Reit E, Gu Y, Fu H, et al. Programmable Acoustic Metasurfaces. Adv Funct Mater. 2019 Mar;29(13):1808489.